Published in final edited form as:
Hepatology. 2011 October ; 54(4): 1282–1292. doi:10.1002/hep.24492.

A protective anti-arrhythmic role of ursodeoxycholic acid in an in-vitro rat model of the cholestatic fetal heart

Michele Miragoli, PhD[1], **Siti H Sheikh Abdul Kadir, PhD**[1], **Mary N. Sheppard, MD**[4], **Nicoló Salvarani, PhD**[2], **Matilda Virta, BS**[1], **Sarah Wells, BS**[1], **Max J. Lab, MD**[1], **Viacheslav O. Nikolaev, PhD**[1], **Alexey Moshkov, PhD**[1], **William M Hague, MD**[5], **Stephan Rohr, MD**[2], **Catherine Williamson, MD**[3], and **Julia Gorelik, PhD**[1]

[1]National Heart and Lung Institute, Imperial College London, London SW3 6LY, UK

[2]Dept. of Physiology, University of Bern, Bühlplatz 5, 3012 Bern, CH

[3]Institute of Reproductive and Developmental Biology, Imperial College London, Du Cane Road, London, W12 0NN, UK

[4]Dept. of Histopathology, Royal Brompton Hospital, Sydney Street London SW3 6NP

[5]Dept of Obstetrics, University of Adelaide, Women's and Children's Hospital, North Adelaide, South Australia 5006, Australia

Abstract

Intrahepatic cholestasis of pregnancy may be complicated by fetal arrhythmia, fetal hypoxia, preterm labour and, in severe cases, intrauterine death. The precise aetiology of the fetal death is not known. However, taurocholate has been demonstrated to cause arrhythmia and abnormal calcium dynamics in cardiomyocytes. To identify the underlying reason for increased susceptibility of fetal cardiomyocytes to arrhythmia we studied myofibroblasts, which appear during structural remodelling of the adult diseased heart. *In-vitro*, they depolarize rat cardiomyocytes via heterocellular gap junctional coupling. Recently, it has been hypothesized that ventricular myofibroblasts might appear in the developing human heart triggered by physiological fetal hypoxia. However, their presence in the fetal heart and their pro-arrhythmogenic effects have not been systematically characterized. Immunohistochemistry demonstrated that ventricular myofibroblasts transiently appear in the human fetal heart during gestation. We established two *in-vitro* models of the maternal and fetal heart both exposed to increasing doses of taurocholate. The maternal heart model consisted of confluent strands of rat cardiomyocytes, while for the fetal heart model we added cardiac myofibroblasts on top of cardiomyocytes. Taurocholate in the fetal heart model, but not in the maternal heart model, slowed the conduction velocity from 19 cm/s to 9 cm/s, induced early afterdepolarizations and resulted in sustained re-entrant arrhythmias. These arrhythmic events were prevented by ursodeoxycholic acid, which hyperpolarized the myofibroblast membrane potential by modulating potassium conductance.

Contact Information: Julia Gorelik, PhD, National Heart and Lung Institute, Imperial College London, Dovehouse street SW36LY London UK. Phone: +44 (0)2073528121 ext: 3324 FAX: +44 (0) 207823 3392 j.gorelik@imperial.ac.uk

Conflict of Interest: None

Europe PMC Funders Author Manuscripts

Conclusion—These results illustrate that the appearance of myofibroblasts in the fetal heart may contribute to arrhythmias. The described mechanism represents a new therapeutic approach for cardiac arrhythmias at the level of myofibroblast.

Keywords

bile acid therapy; intrahepatic cholestasis of pregnancy; fetal arrhythmia; cardiac electrophysiology; heart development

Europe PMC Funders Author Manuscripts

Intrahepatic cholestasis of pregnancy (ICP) is a common disorder presenting in the third trimester of pregnancy.(1) Fetal complications include fetal anoxia, meconium-stained liquor and preterm labour, all occurring more commonly in pregnancies with higher maternal serum bile acids (2). ICP is also associated with fetal arrhythmia (FA)(3, 4) and intrauterine death.(1, 5) Fetal death in ICP affect 2-4% of ICP pregnancies.(6) Interestingly, fetal atrial flutter and supraventricular tachycardia occur in ICP during the second and the third trimester.(3, 4) These FAs may be related to alterations within the cardiac conduction system when seen in pregnancies complicated by maternal disease.(6) Increases in plasma levels of bile acids, in particular taurocholic acid (TC) which has been demonstrated to cross the placental barrier, are probably produced by pathology.(1) We have described the mechanism of TC-induced FA, which was associated with a desynchronization of Ca^{2+} dynamics in cultured neonatal rat cardiomyocytes (CMs), treated with TC that acts as a partial agonist at the muscarinic M_2 receptors.(7) Although fetal complications have been reported in ICP, there are no reports of maternal arrhythmia in affected women. It is still unknown why TC-induced arrhythmia occurs only in the fetal heart (FH) and not in the maternal heart (MH).

The human heart develops in a partially hypoxic environment which is necessary for the normal development of the vasculature and other systems.(8) Moreover, hypoxia is thought to contribute to the *in-vitro* transdifferentiation of human fetal cardiac fibroblasts into myofibroblasts (MFBs).(9) Interstitial MFBs also appear in ischemic, fibrotic and infarcted adult hearts.(10, 11) They are thought to contribute to arrhythmogenesis by excess deposition of extracellular matrix leading to disruption of the orderly 3-dimensional network of electrically coupled CMs. Besides their participation in structural remodelling of diseased hearts, we have recently shown *in-vitro* that MFBs are capable of establishing arrhythmogenic heterocellular gap junctional coupling with CMs, which results in modulation of CMs electrophysiology.(12–14) Therefore, the transient appearance of MFBs in FH might provide a substrate for arrhythmia.

We show here that MFBs transiently appear in human fetal ventricular tissue during the second and the third trimester of gestation, when cholestasis-related sudden fetal death is most common. We therefore explored whether TC induces arrhythmia by investigating cardiac impulse propagation characteristics using a previously described model(13), consisting of a heterocellular preparation of confluent monolayer of CMs coated with a layer of MFBs. For simplicity, this was named the ‘FH model’. Apart from the observation that TC induces arrhythmias under these conditions, we found that ursodeoxycholic acid (UDCA), a commonly used drug to treat ICP, protects against the arrhythmogenic effects of TC by directly affecting the membrane potential (Vm) of MFBs. These findings suggest that

MFBs might be involved in triggering fetal ICP-induced arrhythmia and that these cells possibly represent a new specific target for antiarrhythmic therapy.

Material and Methods

An expanded Methods section is available in the Online Data Supplement

Patterned growth cell cultures of neonatal rat ventricular cardiomyocytes

Isolation procedures from 1-day old Wistar rats were in accordance with the guidelines of the UK Home Office Animal (Scientific Procedures) Act 1986.

Immunocytochemistry

For details see supplemental information

Immunohistochemistry

Human fetal ventricular tissue slices obtained from the Fetal Tissue Bank (Hammersmith, Hospital, London), the postnatal human sample (1-day old) and the adult human infarct (4 month-old) from Dept. of Histopathology, Royal Brompton Hospital, London were stained for alpha smooth muscle actin (α-SMA, Thermo Scientific, Dako), vimentin (Invitrogen) and discoidin domain receptor 2 (DDR2, R&D). Conventional horseradish peroxidase technique was used for immunohistochemical investigations.

Optical and electrical measurement of action potential characteristics

Microscopic measurements of impulse propagation characteristics of the conducted action potentials (APs) were performed using a custom made optical recording system.(15) Macroscopic measurements of electrical activity were performed using a custom built macroscope in conjunction with a fast CMOS camera (Ultima, Scimedia)(14). Vm in monolayer of i) CMs, ii) CM-MFBs, iii) pure MFBs, were measured at 36°C using sharp electrode impalements in selected region of the cell, controlled by a Scanning Ion Conductance Microscope (SICM).(16, 17). Bile acids and glibenclamide were from Sigma.

Data analysis

Data obtained with the macroscopic imaging system were analyzed using proprietary software (Ultima, Scimedia, USA). Microscopic impulse propagation data were analyzed using custom-made software after low-pass filtering the signals (f_0=0.5 kHz). Optically measured action potential amplitudes (APA) were set to 100% (%APA) and maximal upstroke velocities were calculated accordingly (%APA/ms). With an assumed action potential amplitude of 100 mV, %APA/ms corresponds to V/s. Transmembrane potentials were averaged over 1 minute. Based on previous experimental protocols(13) only impalements exhibiting stable potentials for 60-70 sec were analysed (Clampfit 10.0).

Statistics

Data differences were considered significant at $p<0.05$ (*Student's t* test (two-tailed; heteroscedastic)).

Results

Transient appearance of myofibroblasts in human fetal heart tissue during development

We analyzed human ventricular samples derived from fetuses at 9 to 26 weeks of gestation to characterize the presence of MFBs in FH during development. Slices were stained for α-SMA (Figure 1), vimentin and discoidin-domain 2 receptor (Figures S1A-B). Figure 1A shows modest detectable α-SMA expression in the first trimester of gestation. However, during the second and the third trimester α-SMA-positive areas became more defined, showing broader distribution, resulting in a close contact between MFBs and resident CMs. As expected, no MFBs could be detected in postnatal samples, apart from α-SMA positivity within the blood vessels. Quantifying the density of MFBs at different stages of gestation, Figure 1B illustrates that the maximal density of MFBs rises to 17.1% at 15 weeks and with advancing gestation continues ranging between 17.1% and 13.2%. As a positive control, we analyzed a section of i) 6-week-old human healing granulation tissue from a ventricular infarcted area (Figure 1C) and ii) chronically infarcted area induced in rat heart (Figure S1). Both infarct regions are characterized by robust α-SMA positive staining, suggesting the presence of numerous MFBs.

Effects of TC on impulse conduction in the maternal and fetal heart models

Next, we studied the effects of TC using *in-vitro* models of the MH and FH. The healthy adult heart is normally devoid of MFBs. To model this situation *in-vitro*, we constructed homocellular strands of CMs (14) mostly devoid of MFBs (Figure 2, left). For FHs, we added a layer of cardiac MFBs on top of the confluent CM strands that formed a uniform dense coat after 2 days in culture (Figure 2, right). ICP was simulated by exposing MHs and FHs to TC at concentrations typical of severe ICP (0.5 mmol/L, 15 min acute, 12-16 hrs chronic, see supplementary section for case report)(7). Conduction velocity (θ) and maximal upstroke velocities (dV/dt_{max}) were high in the MH model under control conditions (37.1 cm/s, 82.1 %APA/ms) and in the presence of 0.5 mmol/L TC (32.1 cm/s; 81.8 %APA/ms). In contrast, the FH model θ was low (19.8 cm/s) and dV/dt_{max} (43.9 %APA/ms) as previously shown in this heterocellular preparation.(13) Acute administration of TC to the FH model markedly decreased θ from 19.8 cm/s to 9.2 cm/s (lower row, right column) and reduced dV/dt_{max} from 43.9 to 28 %APA/ms. Figure 2B shows a summary of the conduction velocity in the MH and FH models during both acute (10-20 min) and chronic (12-16 h) administration of TC. In the maternal model consisting predominantly of CMs, neither acute nor chronic exposure to TC had any effects on θ (Figure 2B, left). By contrast, acute administration of TC to the FH model reduced θ dose-dependently by ~40% and with chronic administration by ~52% (Figure 2B, right).

In addition, we tested the hypothesis that elevated TC might affect automaticity in the FH model (consisting of a 1cm diameter disc shaped isotropic monolayers of CMs coated with MFBs). Spontaneous activity was measured for 4 seconds using the macroscopic recording system (Figure 3). Electrical impulses in control samples originated from the periphery of the monolayer and propagated uniformly with θ=21cm/s (Figure 3A). After addition of 0.5 mmol/L TC for 10 minutes (Figure 3B), θ was significantly reduced to ~9 cm/s and propagated APs displayed early afterdepolarization (EAD). In the particular experiment

shown, the establishment of sustained re-entrant activity displaying a rotation frequency of 5.2 Hz (movie 01) followed these EADs.

UDCA rescues TC-induced slow conduction

We have previously demonstrated that 0.1 mmol/L UDCA re-synchronizes arrhythmic cardiac calcium dynamics induced by 1 mmol/L TC.(18) We investigated the effect of UDCA alone and in combination with TC on impulse propagation characteristics the MH and FH model. Figure 4A shows that chronic exposure to either 0.1 μmol/L or 1 μmol/L UDCA had no effect on θ in MH models. However, in the FH model, UDCA at concentrations from 0.1 μmol/L to 100 μmol/L increased θ significantly, as compared to untreated strands (Figure 4B). Interestingly, the lowest concentration of UDCA (0.1 μmol/L) maximally improved θ. We next studied whether UDCA not only improves θ but also protects the FH model from arrhythmias induced by either acute or chronic exposure to pathologically relevant concentrations of TC (0.5 mmol/L) (Figure 4C, D). In the FH model exposed to TC either acutely or chronically, 0.1 μmol/L UDCA mitigated the reduction of θ and, as a result, protected against the development of arrhythmias (movie 02). Following acute or chronic administration of TC plus UDCA, θ remained virtually unchanged (Figures 4C-D). Interestingly, in preparations that underwent chronic pre-treatment with UDCA, but from which UDCA was withdrawn before addition of TC, protection against the slow conduction induced by TC was lost (Figure 4D). This indicates that the continuous presence of UDCA and not the treatment itself is a prerequisite for cardioprotection. Table 1 shows a summary of the changes in impulse conduction characteristics in the MH and FH models. Under acute conditions, increasing TC from 0.1 mmol/L to 0.5 mmol/L, led to i) a decay of θ by up to 40.6%, ii) a decay of dV/dt_{max} by up to 19.3% and iii) a decay of Vm by up to 28.1%. During chronic administration of TC, these parameters were further reduced which corroborates the toxic effect of constant exposure to TC. In contrast, the presence of 0.1 μmol/L UDCA during both acute and chronic administration of TC produced a recovery of θ, dV/dt_{max} and Vm.

Mechanism of UDCA-induced cardioprotection

To understand the mechanisms of UDCA-induced cardioprotection in the FH model, we measured resting Vm using SICM in i) the MH model, ii) the FH model and iii) in MFB monolayers where the contamination by CMs was < 1%, as shown by double immunostaining for desmin (green, CMs) and vimentin (red, fibroblastic cells, Figure 5A). While microelectrode impalements in MH and FH models were straightforward due to the models' substantial thickness, this was not the case for the flat MFB monolayers. To facilitate impalement, we first used hopping mode SICM(17) and scanned a membrane region of 80x80 μm, to image the surface topography of the MFB monolayers (Figure 5B). MFBs were mostly flat when forming a monolayer but some regions, presumably located above nuclei, were raised. We chose the highest point on a cell and used the same nanopipette for impalement and measurement of Vm.

We found that acute exposure to 0.1 μmol/L UDCA did not significantly affect Vm in the MH and in FH models. However, in pure MFB monolayers, Vm significantly hyperpolarized from -28.2 mV to -41.9 mV (Figure 5C). Notably chronic exposure to 0.1 μmol/L UDCA

did not affect Vm in the FH model but significantly hyperpolarized the FH model from -54.3 mV to -64.6 mV, and MFB monolayers from -25.5 mV to -44.7 mV (Figure 5D, Figure 6A). We also demonstrate that glibenclamide (5 μmol/L), which binds to the sulfonylurea receptors (SUR), completely abolished the effect of UDCA on the Vm of MFBs (Figure 6A). This suggests that UDCA-induced cardioprotection was dependent on a myofibroblast-specific increase in potassium conductance. In our view, K_{ATP} channels are the most likely candidates, since sulfonylurea at the tested concentrations have been shown to be specific for K_{ATP} channels. Other currents present in the heart such as I_{K1} or I_{Ca} are affected by a concentration of sulfonylurea nearly 10 times higher than the one shown to reduce $I_{K(ATP)}$ by 50%(19). To address directly this hypothesis, we performed radioligand binding experiments with [^{3}H]-glibenclamide and MFB on cell membranes and demonstrated that UDCA can actively displace the radioligand from the SUR with an apparent half-maximal displacement at ~0.1 μmol/L (Figure 6B). This suggests that UDCA can directly bind to SUR, known to be over-expressed in cardiac MFBs(20), thereby regulating potassium conductance.

Discussion

Our results obtained in the MH and FH models strongly suggest that MFBs play a pivotal role in the development of FAs during ICP and may provide an interesting and novel therapeutic target. The results also show that UDCA is a potential antiarrhythmic agent for treating FA (and, possibly, for arrhythmia in adult hearts.) In particular, this study shows that: (i) during gestation, MFBs transiently appear in the heart; (ii) TC at concentrations comparable to those found in ICP provokes arrhythmogenesis and establishes re-entrant activity; (iii) UDCA protects against ICP-induced arrhythmia by directly hyperpolarizing MFBs.

Myofibroblasts in fetal human hearts

MFBs, also described as a ‘scarring phenotype’, are cells present in fibrotic (10) and infarcted regions of the heart.(21) They are likely to contribute to arrhythmogenesis by inducing non-uniform discontinuous conduction following excess deposition of extracellular matrix. Furthermore, they affected the Vm of coupled CMs *in-vitro*, slowing conduction and reducing ectopic activity.(13, 14, 22) Oxygen levels play a key role for fibroblast transdifferentiation. While mouse adult cardiac fibroblasts cultured at 21% O_2 expressed *de-novo* α-SMA,(23) another study found no expression of α-SMA in human fetal cardiac and lung fibroblasts under the same conditions.(9) We found that irregular α-SMA positive regions appear in the human FH at 9 weeks (1.31%) becoming more abundant at the second and the third trimesters when ICP occurs (17.1%). Note that α-SMA positive regions also stain positive for vimentin and DDR2 indicating that they are populated by non-cardiac cells (MFBs). This is of relevance to ICP since the disorder typically presents in the third trimester. Moreover, we previously demonstrated *in-vitro* that MFB-induced arrhythmogenic ectopic activity occurs when the density of MFBs is >15.7%(14) corresponding, according to immunohistochemistry results, to the tissue abundance of MFBs at 15-to-26 weeks of gestation. Although previous studies indicate that α-SMA is transiently expressed during the early stage of the fetal life(24, 25), another study(26) has shown no α-SMA positivity and

fibrosis in septal and ventricular FH at 22 weeks of gestation. Nonetheless, the fetal MFB phenotype is transient, since MFBs are found neither in postnatal nor adult hearts. This transition may vary from heart to heart and can relate not only to the state of hypoxia but also to MFB apoptosis, known to be the key to MFB turnover in cardiac valve development.(27) This is in contrast to infarcted hearts, where the myofibroblast phenotype persists for years.(28) The abundance of MFBs in FH tissue at later stages of gestation and the defined border zone, denote an intimate contact between the two cell populations, which could permit establishment of heterocellular gap junctions. However, as is the case for myofibroblasts in infarcted hearts, this has not been directly demonstrated *in-vivo* so far.

Myofibroblasts and arrhythmia in intrahepatic cholestasis of pregnancy

FA is found in as many as 2% of all pregnancies.(29) Less than 10% of fetuses are found to have sustained tachyarrhythmias or bradyarrhythmias.(30) The proposed aetiology of FAs is heterogeneous and includes maternal metabolic disease,(31, 32) structural abnormalities(33) and autoimmune disorders.(34) It has previously been shown that MFBs tend to depolarize CMs following the establishment of heterocellular gap junctional coupling and that, as a consequence, affect θ(12, 13) and induce spontaneous ectopic activity.(14, 21) However, it has not been previously addressed whether MFB might be involved in ICP related FAs. We use a previously described in-vitro model (14) consisting of i) monolayer strands of CMs (a simplified model of the adult MH devoid of MFBs) or ii) monolayer strands of CMs covered with a layer of cardiac MFBs (a simplified model of FH in the third trimester of gestation). The experimental conditions, i.e. CM isolation and seeding, superfusion solutions, are similar to that previously reported(12–14, 35). In the present study, we added TC to the MH model to generate an *in-vitro* model of ICP that mimics the increase of TC in the bloodstream of pregnant mothers.(36) In addition, to pruritus and chronic hepatitis, such an increase may also cause cardiac dysrhythmia(37) and unexplained stillbirth. Recently, we have described that TC induces arrhythmia in cultured single isolated CMs by targeting calcium dynamics via the muscarinic M_2 receptor.(7) The data presented here suggest that this mechanism of TC-induced arrhythmia does not apply to the MH model consisting of strands of confluent CMs. This is likely related to the fact that CMs coupled electrotonically to neighbouring CMs in a confluent monolayer behave differently to single isolated CMs(14). Whereas single unloaded CMs can be expected to fire APs whenever Vm is disturbed to any significant degree (e.g., Ca^{2+} surge under Ca^{2+} overload conditions), similar excitations are suppressed in an electrotonically coupled network of CMs since individual cells are clamped to a common resting potential. In the FH model, however, TC aggravates slow conduction in a concentration dependent manner by probably affecting the calcium based propagation which is a major determinant of impulse conduction in these partially depolarized preparations.(13) TC induced slowing of θ and dV/dt_{max} was accompanied by a further depolarization (table 1). This slowing of θ, together with the precipitation of EADs, ultimately gave rise to re-entrant electrical activity. The effects of TC on the electrophysiological parameters of the preparations was more pronounced during chronic than during acute administration and revealed a threshold for adverse effects on θ, dV/dt_{max} and Vm at TC >0.3 mmol/L.

Cardioprotective role of UDCA

UDCA treats pruritus and hepatic dysfunction accompanying ICP.(38) Our study shows for the first time that the effect of UDCA on impulse propagation characteristics depends upon the presence of MFBs (Figure 5). Chronic exposure of the FH model to UDCA ranging from 0.1 μmol/L to 100 μmol/L enhanced θ roughly twofold. Acutely administered, UDCA partially counteracted the effects of TC on θ, dV/dt_{max}. In contrast, chronically administered UDCA completely abolished the effect of 0.5 mmol/L TC, indicating a long-term effect on ion channels involved in conduction. Pre-treatment of the preparations with UDCA before TC addition could not elicit this rescuing effect, but it was dependent upon the simultaneous presence of UDCA and TC. Regarding the mechanism underlying the observed UDCA effect, we found that neither acute nor chronic incubation with UDCA changed the diastolic Vm in the MH model, while it produced a substantial hyperpolarization in the FH model. This suggests that UDCA directly targets MFBs. MFBs are cells with a low resting Vm (see Figure 5 and Figure 6A),(13) which is subject to modulation by axial stretch(39), hypoxia(40), and humoral activity.(41) Our data show that UDCA is another modulator of myofibroblast Vm causing hyperpolarization both during acute and chronic application. One possible mechanism underlying hyperpolarization relates to an increase in potassium conductance by direct binding of UDCA to the sulfonylurea receptor expressed in cardiac MFBs (20) and is associated with various Kir and K_{ATP} subunits. Note that in MFB coated CMs strands, opening of K_{ATP} channels increases the degree of polarization and invariably stops arrhythmogenic spontaneous activity(14). In our study, even if K_{ATP} and Kir subunits are known to be present in CMs, UDCA exposure does not further hyperpolarize the well-polarized CMs monolayer. Nevertheless, our finding of a hyperpolarization of a MFBs monolayer after exposure to UDCA suggests that such a cellular compartment is affected and hence contributes to the overall anti-arrhythmic effect of UDCA. Apart from a few studies, demonstrating that some aspects of fetal outcome may be improved in ICP patients receiving UDCA compared to placebo or cholestyramine therapy,(42, 43) the safety and the fetal benefit has not been adequately tested. A pilot study for a trial regarding the fetal benefit of UDCA is currently ongoing, recruiting cholestatic women in six centres.(44) The fetus is recognized as a patient within a patient; therefore, every pharmacological treatment targeting FA may affect also the healthy MH. Our findings demonstrate that UDCA can protect indirectly against ICP-induced arrhythmogenesis by affecting MFBs, which are transiently present only in the FH. Thus, the findings of the present study might be significant for the clinical use of UDCA since they reveal new mechanisms and a possible new strategy for prevention of fetal cardiac arrhythmia.

Study limitations

Although the presence of MFBs in the ventricles of the human FH in the second and third trimester is clearly demonstrated by the expression of α-SMA, further studies are required to characterise their appearance throughout gestation. The scarcity of human fetal cardiac tissue at later gestational weeks limits this approach. Moreover, it is still unclear which role MFBs might play during structural development of the heart and at which stage of gestation they disappear, since they are not present in newborn human hearts, except for the cardiac valve leaflets. Of particular interest and similar to our study, MFBs density was found higher

in cardiac valve development in the second trimester, accompanied by a progressive decrease via apoptosis with advancing gestation.(27)

Therefore, the *in-vitro* model used in this study can only approximate the *in-vivo* pathophysiological situation. In particular, it is not yet known whether MFBs *in-vivo* establish heterocellular electrotonic coupling with CMs. Nevertheless, it has been found that fibroblasts in an infarct scar (known to be MFBs, cf. Figure 1C and (21)) express Cx43 and Cx45,(45) and that MFBs in tissues different from the heart express connexin.(46) These findings suggest, but do not prove, that heterocellular electrotonic coupling is present in the heart. Another limitation of our *in-vitro* model of the FH is that it does not account for the specific 3D-architecture of regions where MFBs intermingle with CMs *in-situ*. Apart from technical difficulties related to the engineering of such structures, there is also a lack of information regarding the exact cytoarchitecture of these regions of the heart.

Conclusion and study implications

The results of the present study raise the possibility that the transient appearance of MFBs in the fetal heart may increase the likelihood of FA during ICP. In general, fetal cardiac arrhythmia is treated with conventional anti-arrhythmic drugs, which may have an adverse effect on the maternal heart. Accordingly, UDCA may represent a new and specific therapeutic role in the management of FA. Indeed, UDCA therapy for ICP, aimed at improving serum bile acid levels, improves some aspects of the fetal outcome. It remains to be investigated whether the benefit on fetal cardiac electrophysiological parameters mediated by myofibroblasts might also be involved in this benefit to the fetus.

Supplementary Material

Refer to Web version on PubMed Central for supplementary material.

Acknowledgments

We thank Christian Dees for radioligand binding assays, and Regula Flueckiger-Labrada for her expert technical assistance. We also acknowledge the encouragement and the enthusiasm by the late Professor Philip Poole-Wilson.

Financial Support: This study was supported by the Action Medical Research (P11880 to J.G and C.W), the Wellcome Trust (P14280 to J.G. and P26660 to J.G.), the Biomedical Research Centre at Imperial College Healthcare NHS Trust and by Swiss National Science Foundation (3100AO-105916 to S.R).

List of Abbreviations

MFBs	myofibroblasts
CMs	cardiomyocytes
ICP	intrahepatic cholestasis of pregnancy
TC	taurocholic acid
FH	fetal heart
MH	maternal heart

UDCA	ursodeoxycholic acid
α-SMA	alpha smooth muscle actin
DDR2	discoidin domain receptor 2
SICM	Scanning Ion Conductance Microscopy
APA	action potential amplitudes
SUR	sulfonylurea receptors
FA	Fetal arrhythmia
Vm	membrane potential
θ	conduction velocity
dV/dt_{max}	maximal upstroke velocities
EAD	early afterdepolarization

References

1. Geenes V, Williamson C. Intrahepatic cholestasis of pregnancy. World J Gastroenterol. 2009; 15:2049–2066. [PubMed: 19418576]
2. Glantz A, Marschall HU, Lammert F, Mattsson LA. Intrahepatic cholestasis of pregnancy: a randomized controlled trial comparing dexamethasone and ursodeoxycholic acid. Hepatology. 2005; 42:1399–1405. [PubMed: 16317669]
3. Al Inizi S, Gupta R, Gale A. Fetal tachyarrhythmia with atrial flutter in obstetric cholestasis. Int J Gynaecol Obstet. 2006; 93:53–54. [PubMed: 16527280]
4. Shand AW, Dickinson JE, D'Orsogna L. Refractory fetal supraventricular tachycardia and obstetric cholestasis. Fetal Diagn Ther. 2008; 24:277–281. [PubMed: 18765943]
5. Fisk NM, Storey GN. Fetal outcome in obstetric cholestasis. Br J Obstet Gynaecol. 1988; 95:1137–1143. [PubMed: 3207643]
6. Strehlow SL, Pathak B, Goodwin TM, Perez BM, Ebrahimi M, Lee RH. The mechanical PR interval in fetuses of women with intrahepatic cholestasis of pregnancy. Am J Obstet Gynecol. 2010 In Press.
7. Sheikh Abdul Kadir SH, Miragoli M, Abu-Hayyeh S, Moshkov AV, Xie Q, Keitel V, Nikolaev VO, et al. Bile acid-induced arrhythmia is mediated by muscarinic M2 receptors in neonatal rat cardiomyocytes. PLoS One. 2010; 5:e9689. [PubMed: 20300620]
8. Webster WS, Abela D. The effect of hypoxia in development. Birth Defects Res C Embryo Today. 2007; 81:215–228. [PubMed: 17963271]
9. Clancy RM, Zheng P, O'Mahony M, Izmirly P, Zavadil J, Gardner L, Buyon JP. Role of hypoxia and cAMP in the transdifferentiation of human fetal cardiac fibroblasts: implications for progression to scarring in autoimmune-associated congenital heart block. Arthritis Rheum. 2007; 56:4120–4131. [PubMed: 18050204]
10. Clement S, Chaponnier C, Gabbiani G. A subpopulation of cardiomyocytes expressing alpha-skeletal actin is identified by a specific polyclonal antibody. Circ Res. 1999; 85:e51–58. [PubMed: 10559147]
11. Sun Y, Kiani MF, Postlethwaite AE, Weber KT. Infarct scar as living tissue. Basic Res Cardiol. 2002; 97:343–347. [PubMed: 12200633]
12. Gaudesius G, Miragoli M, Thomas SP, Rohr S. Coupling of cardiac electrical activity over extended distances by fibroblasts of cardiac origin. Circ Res. 2003; 93:421–428. [PubMed: 12893743]

13. Miragoli M, Gaudesius G, Rohr S. Electrotonic modulation of cardiac impulse conduction by myofibroblasts. Circ Res. 2006; 98:801–810. [PubMed: 16484613]
14. Miragoli M, Salvarani N, Rohr S. Myofibroblasts induce ectopic activity in cardiac tissue. Circ Res. 2007; 101:755–758. [PubMed: 17872460]
15. Rohr S, Kucera JP. Optical recording system based on a fiber optic image conduit: assessment of microscopic activation patterns in cardiac tissue. Biophys J. 1998; 75:1062–1075. [PubMed: 9675208]
16. Nikolaev VO, Moshkov A, Lyon AR, Miragoli M, Novak P, Paur H, Lohse MJ, et al. Beta2-adrenergic receptor redistribution in heart failure changes cAMP compartmentation. Science. 2010; 327:1653–1657. [PubMed: 20185685]
17. Miragoli M, Moshkov A, Novak P, Shevchuk A, Nikolaev VO, El-Hamamsy I, Potter CM, et al. Scanning ion conductance microscopy: a convergent high-resolution technology for multi-parametric analysis of living cardiovascular cells. J R Soc Interface. 2011
18. Gorelik J, Shevchuk AI, Diakonov I, de Swiet M, Lab M, Korchev Y, Williamson C. Dexamethasone and ursodeoxycholic acid protect against the arrhythmogenic effect of taurocholate in an in vitro study of rat cardiomyocytes. BJOG. 2003; 110:467–474. [PubMed: 12742331]
19. Belles B, Hescheler J, Trube G. Changes of membrane currents in cardiac cells induced by long whole-cell recordings and tolbutamide. Pflugers Arch. 1987; 409:582–588. [PubMed: 2442716]
20. Benamer N, Moha Ou Maati H, Demolombe S, Cantereau A, Delwail A, Bois P, Bescond J, et al. Molecular and functional characterization of a new potassium conductance in mouse ventricular fibroblasts. J Mol Cell Cardiol. 2009; 46:508–517. [PubMed: 19166858]
21. Rohr S. Myofibroblasts in diseased hearts: new players in cardiac arrhythmias? Heart Rhythm. 2009; 6:848–856.
22. Chilton L, Ohya S, Freed D, George E, Drobic V, Shibukawa Y, Maccannell KA, et al. K+ currents regulate the resting membrane potential, proliferation, and contractile responses in ventricular fibroblasts and myofibroblasts. Am J Physiol Heart Circ Physiol. 2005; 288:H2931–2939. [PubMed: 15653752]
23. Roy S, Khanna S, Bickerstaff AA, Subramanian SV, Atalay M, Bierl M, Pendyala S, et al. Oxygen sensing by primary cardiac fibroblasts: a key role of p21(Waf1/Cip1/Sdi1). Circ Res. 2003; 92:264–271. [PubMed: 12595337]
24. Suurmeijer AJ, Clement S, Francesconi A, Bocchi L, Angelini A, Van Veldhuisen DJ, Spagnoli LG, et al. Alpha-actin isoform distribution in normal and failing human heart: a morphological, morphometric, and biochemical study. J Pathol. 2003; 199:387–397. [PubMed: 12579541]
25. Potta SP, Liang H, Winkler J, Doss MX, Chen S, Wagh V, Pfannkuche K, et al. Isolation and functional characterization of alpha-smooth muscle actin expressing cardiomyocytes from embryonic stem cells. Cell Physiol Biochem. 2010; 25:595–604. [PubMed: 20511704]
26. Clancy RM, Kapur RP, Molad Y, Askanase AD, Buyon JP. Immunohistologic evidence supports apoptosis, IgG deposition, and novel macrophage/fibroblast crosstalk in the pathologic cascade leading to congenital heart block. Arthritis Rheum. 2004; 50:173–182. [PubMed: 14730614]
27. Aikawa E, Whittaker P, Farber M, Mendelson K, Padera RF, Aikawa M, Schoen FJ. Human semilunar cardiac valve remodeling by activated cells from fetus to adult: implications for postnatal adaptation, pathology, and tissue engineering. Circulation. 2006; 113:1344–1352. [PubMed: 16534030]
28. Weber KT. Fibrosis and hypertensive heart disease. Curr Opin Cardiol. 2000; 15:264–272. [PubMed: 11139090]
29. Cullen T. Evaluation of fetal arrhythmias. Am Fam Physician. 1992; 46:1745–1749. [PubMed: 1456197]
30. Kleinman CS, Nehgme RA. Cardiac arrhythmias in the human fetus. Pediatr Cardiol. 2004; 25:234–251. [PubMed: 15360116]
31. Pusl T, Beuers U. Intrahepatic cholestasis of pregnancy. Orphanet J Rare Dis. 2007; 2:26. [PubMed: 17535422]
32. Kramer DC, Fleischer FS, Marx GF. Fetal bradycardia resulting from maternal hypoglycemia. A report of two cases. J Reprod Med. 1995; 40:394–396. [PubMed: 7608884]

33. Van Gaever C, Defoort P, Dhont M. Delayed structural development in an acardiac fetus: an echographic observation. Fetal Diagn Ther. 2008; 23:100–104. [PubMed: 18033965]
34. Buyon JP, Clancy RM, Friedman DM. Cardiac manifestations of neonatal lupus erythematosus: guidelines to management, integrating clues from the bench and bedside. Nat Clin Pract Rheumatol. 2009; 5:139–148. [PubMed: 19252519]
35. Rohr S, Fluckiger-Labrada R, Kucera JP. Photolithographically defined deposition of attachment factors as a versatile method for patterning the growth of different cell types in culture. Pflugers Arch. 2003; 446:125–132. [PubMed: 12690471]
36. Gorelik J, Harding SE, Shevchuk AI, Koralage D, Lab M, de Swiet M, Korchev Y, et al. Taurocholate induces changes in rat cardiomyocyte contraction and calcium dynamics. Clin Sci (Lond). 2002; 103:191–200. [PubMed: 12149111]
37. Geenes V, Williamson C. Intrahepatic cholestasis of pregnancy. World J Gastroenterol. 2009; 15:2049–2066. [PubMed: 19418576]
38. Glantz A, Reilly SJ, Benthin L, Lammert F, Mattsson LA, Marschall HU. Intrahepatic cholestasis of pregnancy: Amelioration of pruritus by UDCA is associated with decreased progesterone disulphates in urine. Hepatology. 2008; 47:544–551. [PubMed: 17968976]
39. Kamkin A, Kiseleva I, Lozinsky I, Scholz H. Electrical interaction of mechanosensitive fibroblasts and myocytes in the heart. Basic Res Cardiol. 2005; 100:337–345. [PubMed: 15822004]
40. Kamkin A, Kiseleva I, Wagner KD, Lozinsky I, Gunther J, Scholz H. Mechanically induced potentials in atrial fibroblasts from rat hearts are sensitive to hypoxia/reoxygenation. Pflugers Arch. 2003; 446:169–174. [PubMed: 12739154]
41. Chilton L, Giles WR, Smith GL. Evidence of intercellular coupling between co-cultured adult rabbit ventricular myocytes and myofibroblasts. J Physiol. 2007; 583:225–236. [PubMed: 17569734]
42. Palma J, Reyes H, Ribalta J, Hernandez I, Sandoval L, Almuna R, Liepins J, et al. Ursodeoxycholic acid in the treatment of cholestasis of pregnancy: a randomized, double-blind study controlled with placebo. J Hepatol. 1997; 27:1022–1028. [PubMed: 9453428]
43. Kondrackiene J, Beuers U, Kupcinskas L. Efficacy and safety of ursodeoxycholic acid versus cholestyramine in intrahepatic cholestasis of pregnancy. Gastroenterology. 2005; 129:894–901. [PubMed: 16143129]
44. Gurung V, Williamson C, Chappell L, Chambers J, Briley A, Broughton Pipkin F, Thornton J. Pilot study for a trial of ursodeoxycholic acid and/or early delivery for obstetric cholestasis. BMC Pregnancy Childbirth. 2009; 9(19)
45. Camelliti P, Devlin GP, Matthews KG, Kohl P, Green CR. Spatially and temporally distinct expression of fibroblast connexins after sheep ventricular infarction. Cardiovasc Res. 2004; 62:415–425. [PubMed: 15094361]
46. Sui GP, Rothery S, Dupont E, Fry CH, Severs NJ. Gap junctions and connexin expression in human suburothelial interstitial cells. BJU Int. 2002; 90:118–129. [PubMed: 12081783]

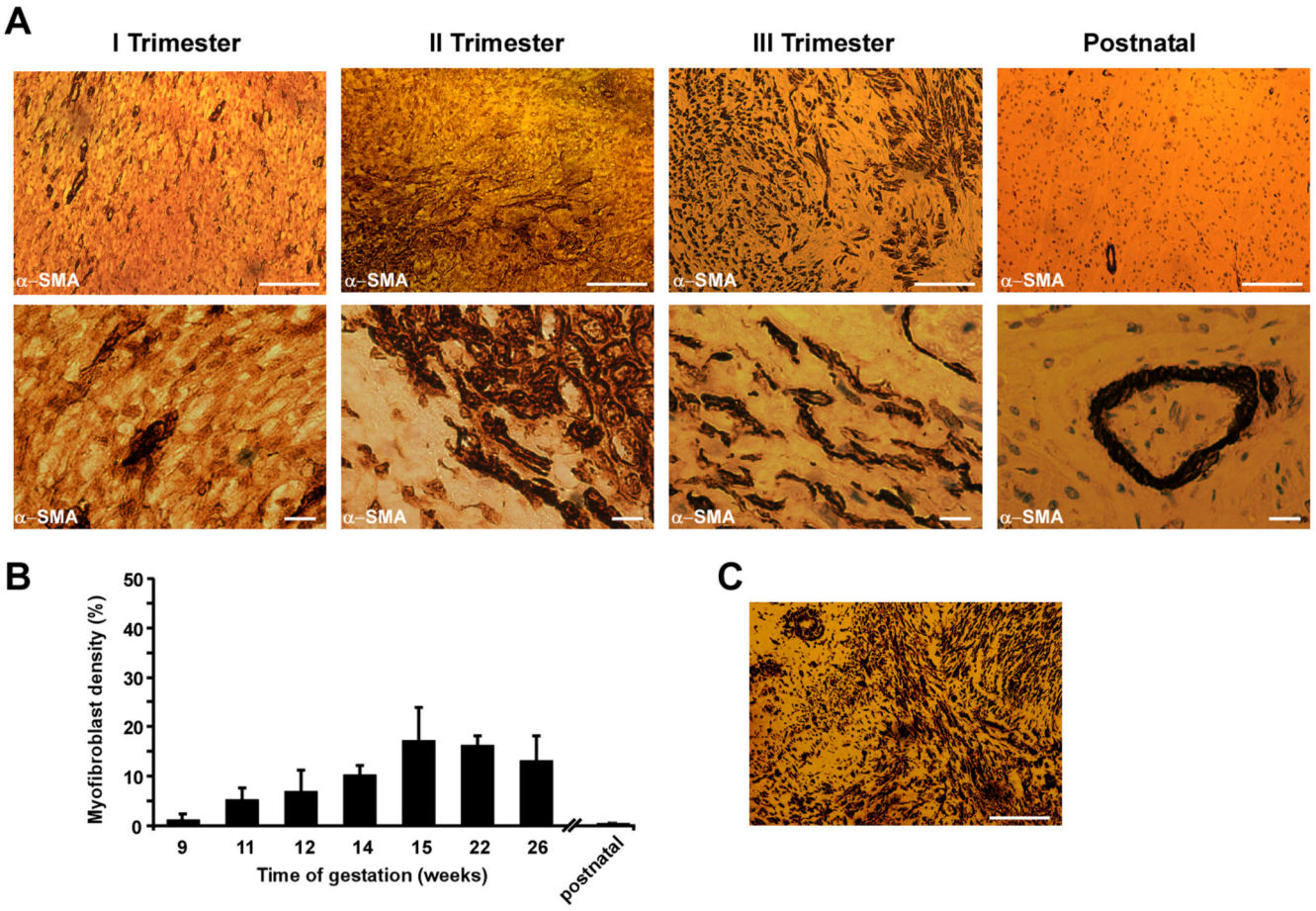

Figure 1.

Immunohistochemical identification of cardiac myofibroblasts in human fetal ventricular tissue slices taken during the three trimesters of gestation. A. Top. Human fetal ventricular myofibroblasts react positively to α-SMA staining, showing scattered myofibroblasts areas (brown) in the second trimester, which becomes denser in the third trimester of gestation. As expected, the postnatal human heart does not contain α-SMA positive cells. Bar=100μm. Bottom. High magnification pictures depict distinct interstitial myofibroblasts (brown) in contact with resident ventricular cardiomyocytes. In postnatal samples, the α-SMA positivity is related to smooth-muscle cells lining the blood vessels. Bar=10μm. B. Transient increment of myofibroblast density throughout gestation. Myofibroblast density was analyzed from fixed ventricular preparations derived from a single fetal heart corresponding to each week of gestation, (n=10 random locations). Data: means±SD.

C. Staining of infarcted human heart 6 weeks-old granulation tissue. Positive staining for α-SMA (brown) indicates presence of abundant myofibroblasts. Bar=100μm.

Europe PMC Funders Author Manuscripts

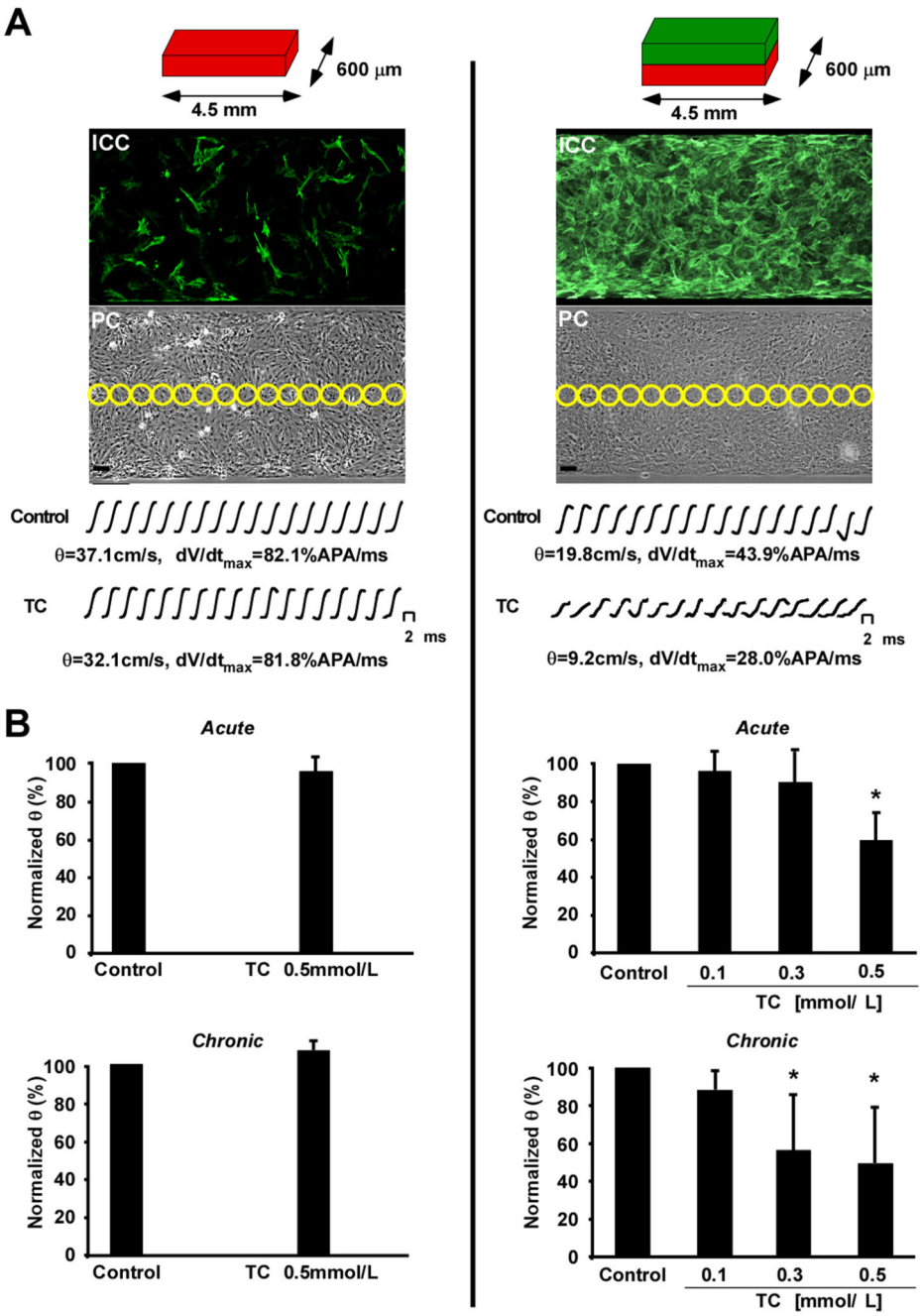

Figure 2.

Optical recording of impulse propagation along homo- and heterocellular cell strands. A. Left column. Schematic representation of the maternal heart model (MH, red) consisting of strands of neonatal rat cardiomyocytes (0.6 × 4.5 mm) with little myofibroblast contamination as illustrated by the anti α-SMA staining in the immunocytochemistry (ICC) picture. Yellow circles in the corresponding phase contrast image (PC) indicate the positions of photodetectors used to record electrical activity. Bar=50 μm. Action potential upstrokes recorded during propagated activity were monophasic and fast rising and remained virtually

unchanged during exposure to 0.5 mmol/L taurocholic acid (TC). B. Left column. Neither acute (top) nor chronic (bottom) application of 0.5 mmol/L TC had any significant effects on conduction velocity (θ). A. Right column. Schematic representation of the fetal heart model (FH) having identical dimensions to the maternal heart (MH) but consisting of strands of neonatal rat cardiomyocytes (red) coated with myofibroblasts (green). As indicated by the anti α-SMA staining, myofibroblasts formed a uniform cellular coat. Under control conditions, θ was slow in FH compared to the MH and acute application of 0.5 mmol/L TC led to a substantial reduction of θ and dV/dt_{max}. B. Right column. Both acute (top) and chronic (bottom) application of TC ranging from 0.1 to 0.5 mmol/L reduces θ in a dose dependent manner. Data: means±SD (n=9).

Europe PMC Funders Author Manuscripts

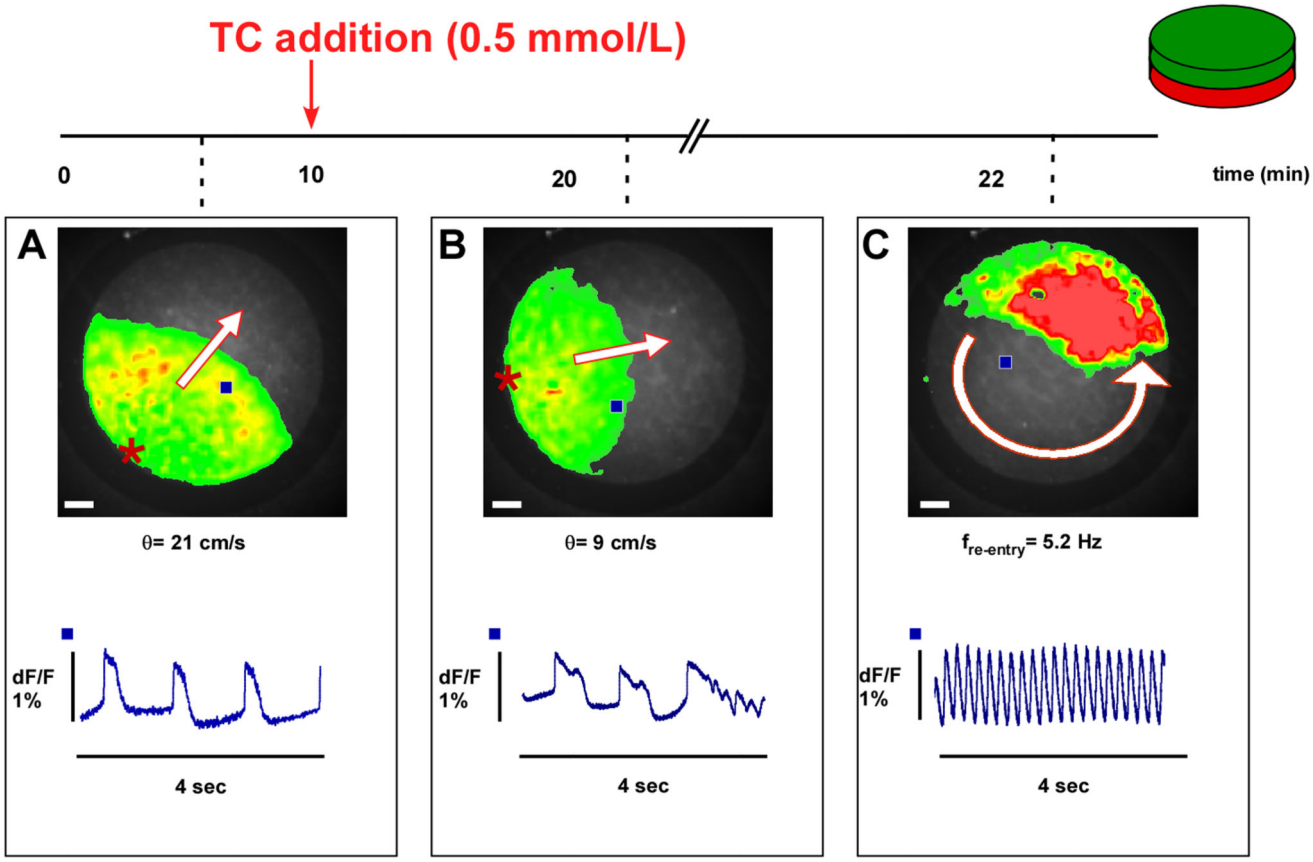

Figure 3.

Example of the arrhythmia induced by taurocholic acid (TC) in a preparation consisting of a monolayer of CMs coated with a monolayer of MFBs. A. Optical recording of spontaneous electrical activity (45 bpm, bottom) originates from the periphery and propagates uniformly at 21 cm/s. B. After acute exposure to 0.5 mmol/L, TC conduction velocity (θ) is reduced from 21 to 9 cm/s. Moreover, propagated APs display early afterdepolarizations where the last activation is followed by (C) self-sustained re-entrant excitation. Frequency of rotation is 5.2 Hz. Bar=1 mm. Blue squares in the overview indicate the locations of recorded traces. Red stars indicate the origins of spontaneous electrical activation.

Europe PMC Funders Author Manuscripts

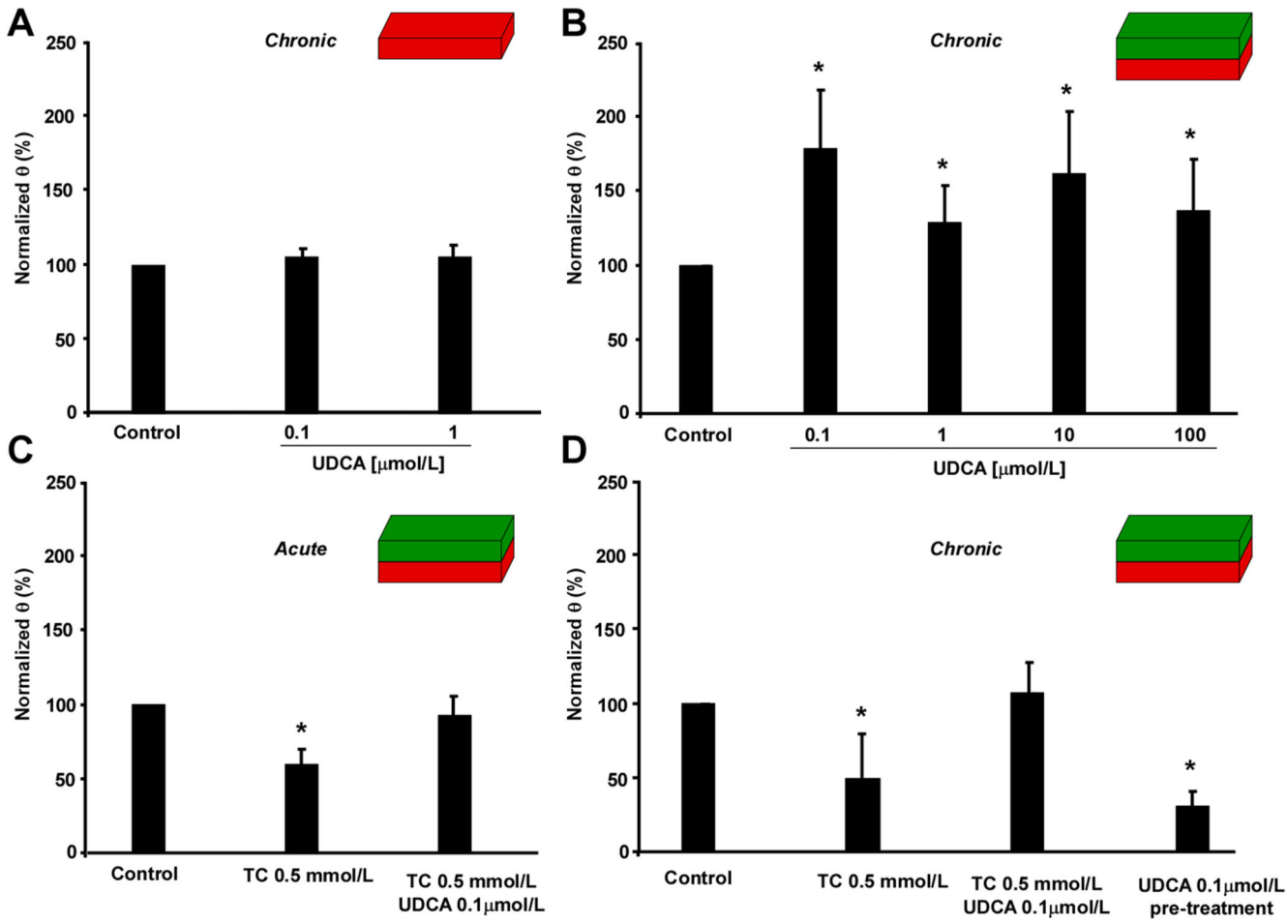

Figure 4.

Effect of exposure to ursodeoxycholic acid (UDCA) on impulse propagation in the maternal (MH) and fetal heart (FH) models. A. Chronic exposure of the MH model to UDCA does not affect conduction velocity (θ, n=7). B. In contrast, chronic exposure of the FH model to increasing concentrations of UDCA significantly increases θ (n=24). C. Acute exposure of FH models to 0.5 mmol/L taurocholic acid (TC) plus 0.1 μmol/L UDCA inhibits slow conduction induced by TC alone (n=7). D. Same as C, but following chronic exposure of FH models to TC and UDCA. Again, UDCA plus TC abolishes slow conduction induced by TC alone. UDCA pre-treatment for 12 hrs (UDCA withdrawn before adding 0.5 mmol/L TC for 12 hrs) shows no cardio-protective effect (n=7). Data: mean±SD.

Europe PMC Funders Author Manuscripts

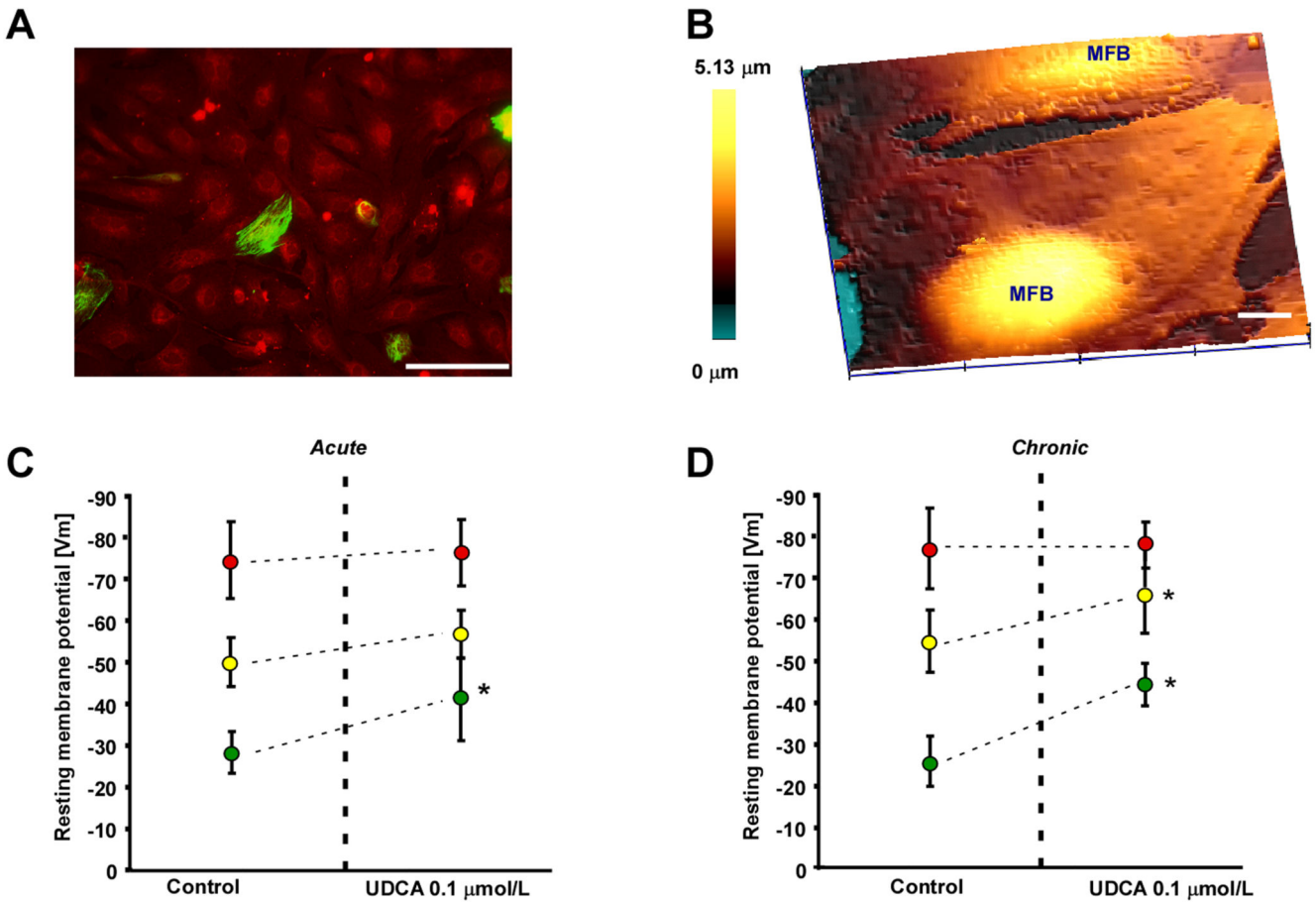

Figure 5.

Effect of ursodeoxycholic acid (UDCA) on membrane potential (Vm) in the maternal heart model (MH), fetal heart model (FH) and myofibroblast monolayers. A. Myofibroblast monolayer stained for desmin (green) and vimentin (red) indicates a low contamination by desmin positive cardiomyocytes. Bar=100 μm. B. Scanning ion conductance microscopy identifies the most prominent area for impalement as regions above nuclei in the myofibroblast monolayer. Bar=10 μm. C. Acute exposure to 0.1 μmol/L UDCA significantly increases Vm only in pure myofibroblast monolayers (green dots) but not in the MH model (red dots) and FH model (yellow dots). D. Same as C for chronic exposure to UDCA. 0.1 μmol/L. UDCA significantly increases Vm in the FH model and myofibroblast monolayers but has no effect on MH model preparations. Data: means±SD, n=12.

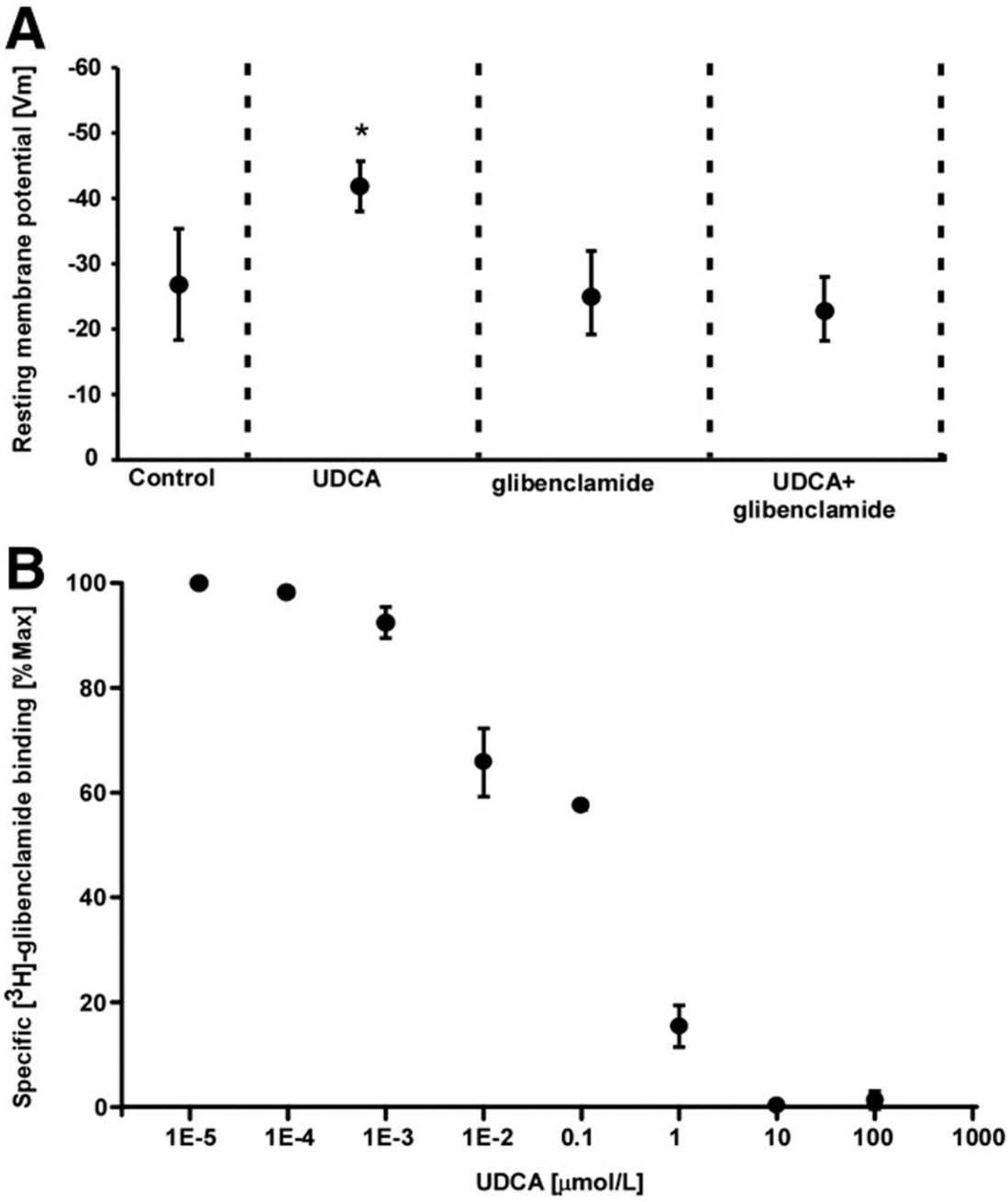

Figure 6.

Ursodeoxycholic acid (UDCA) hyperpolarizes myofibroblasts by increasing potassium conductance. A. Glibenclamide inhibits the effect of UDCA, indicating that UDCA is involved in the modulation of potassium conductance. Data: means±SD, n=12. B. Specific binding of [^{3}H]-glibenclamide to sulphonylureas receptors in myofibroblast membranes is competitively displaced by increasing concentrations of UDCA. Data: means±SE n=3.

Europe PMC Funders Author Manuscripts

Table 1

Effect of Bile Acids on Impulse Conduction Characteristics

Bile Acids		Conduction Velocity, cm/s			Upstroke Velocity, %APA/ms		
		Control	Drug	% change	Control	Drug	% change
TC 0.1mmol/L	ACUTE	24.8±3.0	23.8±1.9	-4.0%	36.1±3.7	33.1±1.4	-8.3%
	CHRONIC	24.6±4.2	21.6±1.5	-11.8%	43.0±7.6	39.4±5.9	-8.2%
TC 0.3mmol/L	ACUTE	17.2±5.7	15.5±2.9	-9.7%	33.1±1.4	29.2±4.3 *	-11.7%
	CHRONIC	17.3±4.3	9.7±2.8 **	-43.8%	42.6±1.5	36.8±5.1 **	-13.4%
TC 0.5mmol/L	ACUTE	17.0±4.3	10.1±1.8 *	-40.6%	47.5±10.8	38.2±2.2 *	-19.3%
	CHRONIC	22.1±3.8	10.8±2.9 **	-51.0%	41.3±5.4	30.8±2.5 *	-25.4%
TC 0.5mmol/L + UDCA0.1 μmol/L	ACUTE	17.6±1.3	16.2±2.2	-7.7%	32.5±0.9	33.1±1.9	+1.7%
	CHRONIC	20.6±4.7	22.1±4.1	+7.1%	43.8±3.1	44.8±2.9	+2.2%

Measured in confluent srands of myofibroblasts-coated cardiomyocytes (n=7 each)

* $P<0.05$ vs. control

** $P<0.005$ vs. control